Physics Letters A 374 (2010) 1527–1533

Contents lists available at ScienceDirect

Physics Letters A

www.elsevier.com/locate/pla

Interactions of fast charged particles with supported two-dimensional electron gas: One-fluid model

Ivan Radović *, Duško Borka

VINČA Institute of Nuclear Sciences, P.O. Box 522, 11001 Belgrade, Serbia

ARTICLE INFO

Article history:
Received 25 November 2009
Received in revised form 14 January 2010
Accepted 25 January 2010
Available online 1 February 2010
Communicated by R. Wu

Keywords:
2D electron gas
Graphene
Stopping force
Image force
Wake effect

ABSTRACT

We investigate the interactions of fast charged particles with a two-dimensional (2D) electron gas (2DEG) supported by an insulating substrate, describing its collective or plasmon excitations by a one-fluid hydrodynamic model with the parameters characteristic of graphene. By linearizing the hydrodynamic equations, we derive general expressions for the induced potential, stopping force and the image force on a particle moving parallel to the 2DEG, as well as for the induced number density per unit area of electrons in the 2DEG. Numerical results are obtained showing the effects of variation in size of the gap between the 2DEG and the SiO_2 substrate on these quantities. It is also found that, when the particle speed exceeds a threshold value for the collective excitations, the oscillatory wake effect develops in the induced number density trailing the particle.

1. Introduction

Renewed interest in the properties of two-dimensional (2D) electron systems is stimulated by recent experimental discovery of graphene, a single sheet of carbon atoms forming hexagonal lattice [1]. One can consider various carbon nanostructures to be composed of interacting layers of 2D electron gas (2DEG) confined to a graphene sheet: highly oriented pyrolytic graphite (HOPG, a stack of graphene layers), carbon nanotubes (rolled-up cylinders of graphene) and fullerene molecules (consisting of wrapped graphene by the introduction of pentagons on the hexagonal lattice) [2,3]. Interactions of fast-moving charged particles with various carbon nanostructures have been investigated in recent years, e.g., in the electron energy loss spectroscopy (EELS) of carbon nanotubes [4] and isolated layers of free-standing graphene [5].

On the other hand, interactions of energetic heavy charged particles with layered materials have been studied extensively for some time, e.g., in investigations of the directional effects in ion and molecule implantation into HOPG [6,7], ion channelling through HOPG [8] and secondary electron emission from HOPG induced by fast ions [9] and clusters [10], as well as in ion channelling through carbon nanotubes [11–13].

In order to better understand particle interactions with layered graphitic nanostructures and motivated by these developments, we explore here the effects of dynamic-polarization forces on fast charges incident upon a planar 2DEG supported by an insulating substrate. Specifically, we calculate the dissipative or stopping force on fast ions moving parallel to the 2DEG and the perpendicularly oriented conservative force on such ions due to the dynamic image interaction. As we all know, the stopping force is very important for energy loss experiments. The importance of the image force was demonstrated recently, e.g., in ion channelling through carbon nanotubes, where it was found to strongly attract ions towards the nanotube walls [13]. Moreover, in the static regime, image force is often responsible for giving rise to the so-called electron image-potential bound states, observed on solid surfaces [14] and around carbon nanotubes [15].

Generally speaking, the easiest way to calculate these forces is based on a 2D hydrodynamic model [16] which proved itself to be a valuable theoretical tool for qualitative understanding of the high-frequency, collective excitations in carbon nanotubes [11,17]. We note that the dynamic-polarization forces on fast ions moving parallel to a 2DEG corresponding to the four valence electrons in graphene can also be calculated using a three-dimensional (3D) hydrodynamic model which uses in the ground-state the electron density obtained from the Thomas–Fermi class of models for graphene in jellium approximation [18]. A direct comparison between the results obtained from the 2D and 3D hydrodynamic models goes beyond the scope of this Letter.

The 2D hydrodynamic model allows many refinements including Thomas–Fermi and Dirac's corrections, as well as a generalization in a two-fluid version, making distinction between the contributions of carbon's σ and π electrons [11,12]. In our previous publication [19] we have calculated the stopping and image forces

* Corresponding author. Tel.: +381 11 3408 672; fax: +381 11 8066 425.
E-mail address: iradovic@vinca.rs (I. Radović).

0375-9601/$ – see front matter
doi:10.1016/j.physleta.2010.01.056

on both ions and molecules by solving the linearized two-fluid hydrodynamic model for a supported graphene. However, since the two-fluid model proved too complex for evaluation of the nonlinear effects, we limited ourselves to a simpler, one-fluid hydrodynamic model, which treats all four carbon's valence electrons as a single 2DEG, to evaluate the stopping and image forces up to the second order, as shown in our previous publication [20]. The one-fluid hydrodynamic model has its own merits. Namely, it was shown that this model provides essentially the same results as the two-fluid model for both the stopping and image forces for charged particles moving at the speeds higher than about Bohr's velocity [11,12]. Consequently, Borka et al. [13,21,22] have used the one-fluid model to evaluate the dynamic image force on protons channelled through carbon nanotubes in the MeV energy range. Therefore, taking advantage of its simplicity, we use here the one-fluid model to provide relatively compact and transparent formulas allowing both easy computation and analytical description of several effects on these forces, such as the dielectric response of a substrate, size of the gap between the 2DEG and the substrate, and the role of finite damping rate of collective electron excitations due to various scattering processes.

The second aim of this Letter is to present the wake effect which is characterized by the onset of collective oscillations in the polarization of the medium, which provide effective mechanisms of energy loss for a fast charged particle. While the wake effect in three-dimensional plasmas has been known for more than fifty years [23], its current significance encompasses diverse new areas, such as dust-crystal formation in complex plasmas [24], Coulomb explosion of large clusters, such as C_{60}, in thin solid foils [25], channelling of fast ions through nano-capillaries in solids [26], interactions of fast ions with carbon nanotubes [11,27] and interactions of charged particles with single two-dimensional quantum electron gases (2DQEG) [28], parallel 2DQEG [29] and supported thin metal films [30]. The results for the wake effect in interactions of fast ions with carbon nanostructures are useful because they indicate a possibility of realizing the so-called wake riding effect [27,31]. It means that the presence of the potential, induced by a fast external charge, causes that the other charged particles may be captured, or their state manipulated.

In this Letter, we describe the high-frequency collective electron excitations in a 2DEG corresponding to the four valence electrons in graphene. As regards graphene, it usually appears in experimental situations as supported by a substrate [32,33]. Surprisingly, all theoretical models of graphene's dynamic response assume a zero gap between the graphene and a substrate [34,35]. In our previous publications we have studied the interactions of slow ions, moving at the speeds below the plasmon excitation threshold for graphene's σ electrons, by means of a semiclassical Vlasov equation for graphene's π electrons [36] and by using the dielectric response formalism for graphene's π electron bands in the random phase approximation (RPA) [37], and pointed to a strong need to take into account the finite size of such a gap, which is on the order of the distance between graphene layers in graphite or even larger, as documented experimentally [33].

In order to deduce the parameter range of applicability of the one-fluid hydrodynamic model for describing the dynamic response of carbon nanostructures to external charges, we note that this model treats 2DEG as a structureless 2D jellium of quasi-free electrons. In that context, the effect of graphene's lattice structure can be neglected by restricting applications of the hydrodynamic model to cases when the 2DEG response is dominated by the plasmon excitations with sufficiently long wavelengths, such that their wavenumbers satisfy the relation $k < 1/a$, where $a \approx 1.42$ Å is the lattice constant of graphene [38]. On the other hand, the effects of band structure can be neglected if the excitation energies in the 2DEG exceed the gap between graphene's σ bands, which is of the order of $\varepsilon_g \approx 7$ eV [38]. Furthermore, using Bohr's adiabatic criterion for a projectile moving at constant velocity v parallel to graphene at distance z_0, one can assert the dynamic range of applicability of the one-fluid hydrodynamic model to be $v/z_0 > \varepsilon_g/\hbar$, where $\hbar$ is the reduced Planck constant. Therefore, one concludes that, for not too large distances z_0, the projectile speed should exceed Bohr's velocity. At such high speeds the dynamic response of carbon nanostructures is dominated by the high-frequency $\sigma + \pi$ plasmon excitations [11,12,17], so that the one-fluid hydrodynamic model provides an adequate basis for calculations of the stopping forces, the image forces and the induced number densities.

We note that the presented hydrodynamic model can be applied to a 2DEG on a curved surface, according Refs. [39–41], provided that its local radius of curvature R far exceeds the inverse of the Fermi wavenumber, $k_F = \sqrt{2\pi n_0}$, where n_0 is the surface density of a 2DEG [42].

In this work, we present for the first time the effects of variation in size of the gap on the stopping and image forces, as well as the effects of a finite frictional coefficient for the 2D one-fluid hydrodynamic model. Besides, we show the influence of the ion position and its velocity on the stopping and image forces. We also present for the first time the oscillatory wake effect which develops in the induced number density when the particle speed exceeds a threshold value for the collective excitations in a 2DEG corresponding to the four valence electrons in graphene. Finally, we present for the first time the influence of the quantum diffraction (QD) effects on the stopping force, the image force and the induced number density. While the configuration of graphene on metal [32] opens interesting possibility of exciting novel modes of collective electron excitations due to plasmon hybridization [12,43], we limit ourselves here to the insulating substrate, such as SiO_2 lying underneath a single graphene sheet [33].

The Letter is organized as follows. After outlining the theoretical model in the following section, we shall present and discuss the results for the stopping and image forces for a range of the relevant parameters, as well as the results for the induced number density. Concluding remarks will be given in the last section.

Atomic units (a.u.) will be used throughout unless indicated otherwise.

2. Basic theory

We use a Cartesian coordinate system with coordinates $\{\vec{R}, z\}$ and assume that the 2DEG is located in the plane $z = 0$, where $\vec{R} = \{x, y\}$ is position in the plane and z distance from it. A substrate with dielectric constant ε_s is assumed to occupy the region $z \leqslant -h$ underneath the 2DEG, whereas the region $z > -h$ is assumed to be vacuum or air. Moreover, we assume that a fast ion of charge Q moves parallel to the 2DEG at a fixed distance $z_0 > 0$ above it with a constant velocity $\vec{v}$, so that its density can be written as $\rho_{ext}(\vec{R}, z, t) = Q\,\delta(\vec{R} - \vec{v}t)\delta(z - z_0)$.

In order to treat the effects of substrate on the dynamic response of a 2DEG to external perturbation, we resort to the method of Doerr and Yu [44]. The same method can be used to treat the effects of a cylindrical cavity in dielectric material on a carbon nanotube grown inside that cavity [12]. Denoting the electric potentials due to charge polarization on the 2DEG and the induced surface charge on the substrate, respectively, by Φ_{gr} and Φ_s, the total electric potential in the system, Φ_{tot}, can be written as the sum

$$\Phi_{tot} = \Phi_{ext} + \Phi_{gr} + \Phi_s \tag{1}$$

where Φ_{ext} is the external perturbing potential. If there are no free charges on the substrate surface, which is assumed to be structureless, one can use the continuity of the normal component of the displacement vector

$$\left.\frac{\partial \Phi_{tot}}{\partial z}\right|_{z=-h+0} = \varepsilon_s \left.\frac{\partial \Phi_{tot}}{\partial z}\right|_{z=-h-0} \tag{2}$$

to obtain the induced charge density on the substrate surface, σ_s [12,19,36,44]. This is easily implemented by using the Fourier transform with respect to coordinates in the xy plane, $\vec{R} \to \vec{k}$, and time, $t \to \omega$, defined by

$$A(\vec{R}, z, t) = \frac{1}{(2\pi)^3} \int A(\vec{k}, z, \omega) e^{-i(\omega t - \vec{k}\cdot\vec{R})}\, d^2\vec{k}\, d\omega \tag{3}$$

for an arbitrary function A, with $\vec{k} = \{k_x, k_y\}$. Then, one obtains

$$\Phi_{ext}(\vec{k}, z, \omega) = \frac{(2\pi)^2 Q\, \delta(\omega - \vec{k}\cdot\vec{v})}{k} e^{-k|z-z_0|} \tag{4}$$

$$\Phi_{gr}(\vec{k}, z, \omega) = -\frac{2\pi}{k} n(\vec{k}, \omega) e^{-k|z|} \tag{5}$$

$$\Phi_s(\vec{k}, z, \omega) = \frac{2\pi}{k} \sigma_s(\vec{k}, \omega) e^{-k|z+h|} \tag{6}$$

where $k = \sqrt{k_x^2 + k_y^2}$ and $n(\vec{k}, \omega)$ is the Fourier transform of the perturbation of the number density per unit area of electrons in the 2DEG.

Next, we consider that the 2DEG in equilibrium is uniformly distributed in the xy plane and has the surface density (density per unit area) of $n_0 = 0.428$ corresponding to the four valence electrons per carbon atom in graphene [38]. The perturbations of its density $n(\vec{R}, t)$ and its velocity field $\vec{u}(\vec{R}, t)$ satisfy the linearized continuity equation

$$\frac{\partial n(\vec{R}, t)}{\partial t} + n_0 \nabla_\parallel \cdot \vec{u}(\vec{R}, t) = 0 \tag{7}$$

and the linearized momentum-balance equation

$$\frac{\partial \vec{u}(\vec{R}, t)}{\partial t} = \nabla_\parallel \Phi_{tot}(\vec{R}, z, t)|_{z=0} - \frac{\alpha}{n_0} \nabla_\parallel n(\vec{R}, t) - \gamma \vec{u}(\vec{R}, t) \tag{8}$$

Note that, in Eqs. (7) and (8), $\nabla_\parallel = \partial/\partial\vec{R}$ is the component of the full gradient operator which differentiates in directions parallel to the sheet. The first term in the right side of Eq. (8) is the tangential force on an electron due to the total electric field at $z = 0$. The second term represents the internal interactions in the electron fluid based on the Thomas–Fermi model [45,46], giving $\alpha = \pi n_0$. The last term in Eq. (8) describes the frictional force on an electron due to scattering on the positive charge background, where γ is the frictional coefficient.

By eliminating the velocity field $\vec{u}(\vec{R}, t)$, one obtains from Eqs. (7) and (8)

$$\left(\frac{\partial^2}{\partial t^2} + \gamma \frac{\partial}{\partial t} - \alpha \nabla_\parallel^2\right) n(\vec{R}, t) = -n_0 \nabla_\parallel^2 \Phi_{tot}(\vec{R}, z, t)|_{z=0} \tag{9}$$

Performing the Fourier transformation in the xy plane and in time ($\vec{R} \to \vec{k}$ and $t \to \omega$) gives a relation between the electron number density in a 2DEG and the local value of the total potential at $z = 0$ in the form

$$n(\vec{k}, \omega) = \chi(k, \omega) \Phi_{tot}(\vec{k}, z, \omega)|_{z=0} \tag{10}$$

where the polarization function of the 2DEG in the one-fluid model is given by

$$\chi(k, \omega) = \frac{n_0 k^2}{\alpha k^2 - \omega^2 - i\gamma\omega} \tag{11}$$

Using the relation (10) along with Eqs. (4), (5) and (6) and the Fourier transforms of the boundary condition (2) and the decomposition of the total potential (1), one can obtain the Fourier transform of the induced potential, $\Phi_{ind} = \Phi_{gr} + \Phi_s$, in the region above a 2DEG ($z > 0$), as follows

$$\Phi_{ind}(\vec{k}, z, \omega) = -\frac{(2\pi)^2 Q e^{-k(z+z_0)}}{k} \left[1 - \frac{1}{\varepsilon(k, \omega)}\right] \delta(\omega - \vec{k}\cdot\vec{v}) \tag{12}$$

where

$$\varepsilon(k, \omega) = \varepsilon_0(k) + \frac{2\pi}{k} \chi(k, \omega) \tag{13}$$

is the dielectric function of supported 2DEG, with

$$\varepsilon_0(k) \equiv \frac{1}{1 - \frac{\varepsilon_s - 1}{\varepsilon_s + 1} e^{-2kh}} \tag{14}$$

being the background dielectric function which quantifies the effects of substrate on the response of the 2DEG. Note that $\varepsilon_0(k)$ takes the values in the range between 1 and $(\varepsilon_s + 1)/2$, characterizing, respectively, the case of a free-standing 2DEG ($h \to \infty$) and the case of a zero gap ($h = 0$) between the 2DEG and a substrate.

We note that the dispersion relation of the system can be obtained from Eq. (13). In contrast to the Nakayama's [47] and Fetter's [48] results, we neglect the retardation effects in the electric field. It means that the dispersion relation is derived in the region $(\omega/k) \ll c$, where c is the speed of light.

Finally, by performing the inverse Fourier transformation in the xy plane and in time ($\vec{k} \to \vec{R}$ and $\omega \to t$), one obtains an expression for the induced potential as follows

$$\Phi_{ind}(\vec{R}, z, t) = -\frac{Q}{2\pi} \int \frac{e^{-k(z+z_0)}}{k} \left[1 - \frac{1}{\varepsilon(k, \vec{k}\cdot\vec{v})}\right] e^{i\vec{k}\cdot(\vec{R} - \vec{v}t)}\, d^2\vec{k} \tag{15}$$

As regards the induced number density, one can obtain, using the relation (10) along with Eqs. (4) and (12), its Fourier transform as follows

$$n(\vec{k}, \omega) = 2\pi\, Q\, \delta(\omega - \vec{k}\cdot\vec{v}) e^{-kz_0} \left[1 - \frac{\varepsilon_0(k)}{\varepsilon(k, \omega)}\right] \tag{16}$$

By performing the inverse Fourier transformation in the xy plane and in time, one obtains, for an ion of charge Q moving along the x axis with speed v at a fixed distance $z_0 > 0$ above a 2DEG, an expression for the induced number density as follows

$$n(x, y, t) = \frac{Q}{\pi^2} \int_0^\infty \int_0^\infty e^{-kz_0} \operatorname{Re}\left\{\left[1 - \frac{\varepsilon_0(k)}{\varepsilon(k, k_x v)}\right] e^{i[k_x(x - vt) + k_y y]}\right\} dk_x\, dk_y \tag{17}$$

where we have used the symmetry properties of the real and imaginary parts of the dielectric function $\varepsilon(k, \omega)$ from Eq. (13).

3. Results and discussion

When studying the energy loss of fast ions moving parallel to a 2DEG, it is important to look at the force which opposes the ion's motion, called the stopping force. The conservative force which bends the ion's trajectory towards the sheet is called the image force. The stopping and image forces are defined in terms of the induced potential, $\Phi_{ind}(\vec{R}, z, t)$, respectively, as follows

$$F_s = -Q \frac{\vec{v}}{v} \cdot \nabla_\parallel \Phi_{ind}(\vec{R}, z, t)|_{\vec{R} = \vec{v}t, z = z_0} \tag{18}$$

$$F_{im} = -Q \left.\frac{\partial \Phi_{ind}(\vec{R}, z, t)}{\partial z}\right|_{\vec{R} = \vec{v}t, z = z_0} \tag{19}$$

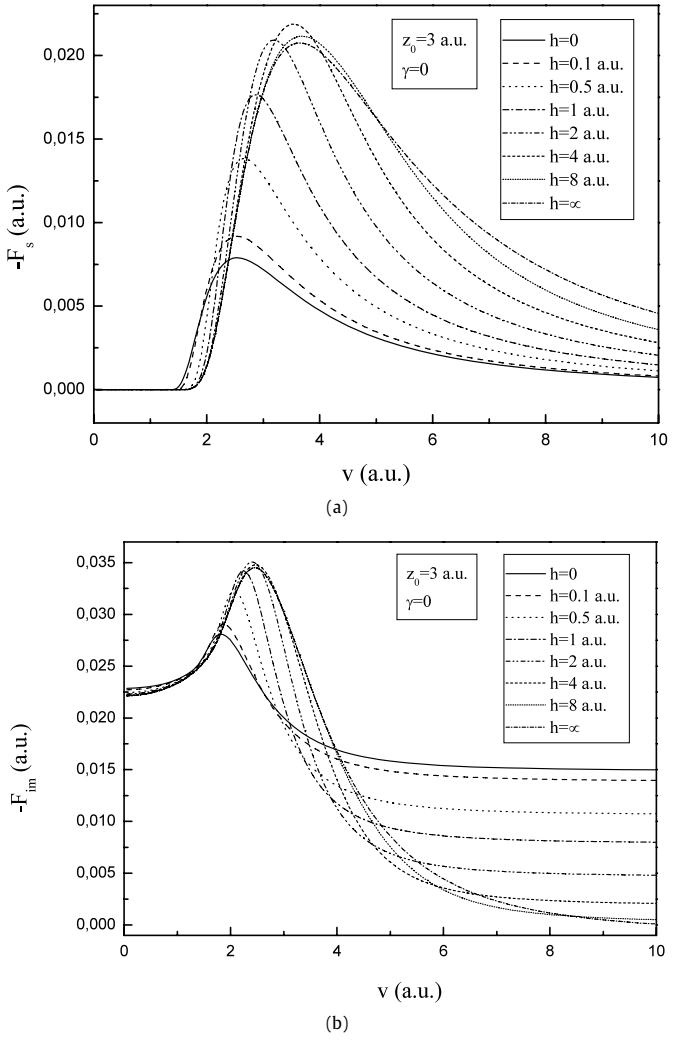

Fig. 1. The dependencies on speed v (in a.u.) of (a) stopping and (b) image forces (in a.u.) on proton moving at distance $z_0 = 3$ a.u. above 2DEG for eight values of the gap between 2DEG and a SiO_2 substrate (with $\varepsilon_s = 3.9$), $h = 0$ (solid lines), 0.1 a.u. (dashed lines), 0.5 a.u. (dotted lines), 1 a.u. (dash-dotted lines), 2 a.u. (dash-dot-dotted lines), 4 a.u. (short dashed lines), 8 a.u. (short dotted lines) and ∞ (short dash-dotted lines), with zero damping $\gamma = 0$.

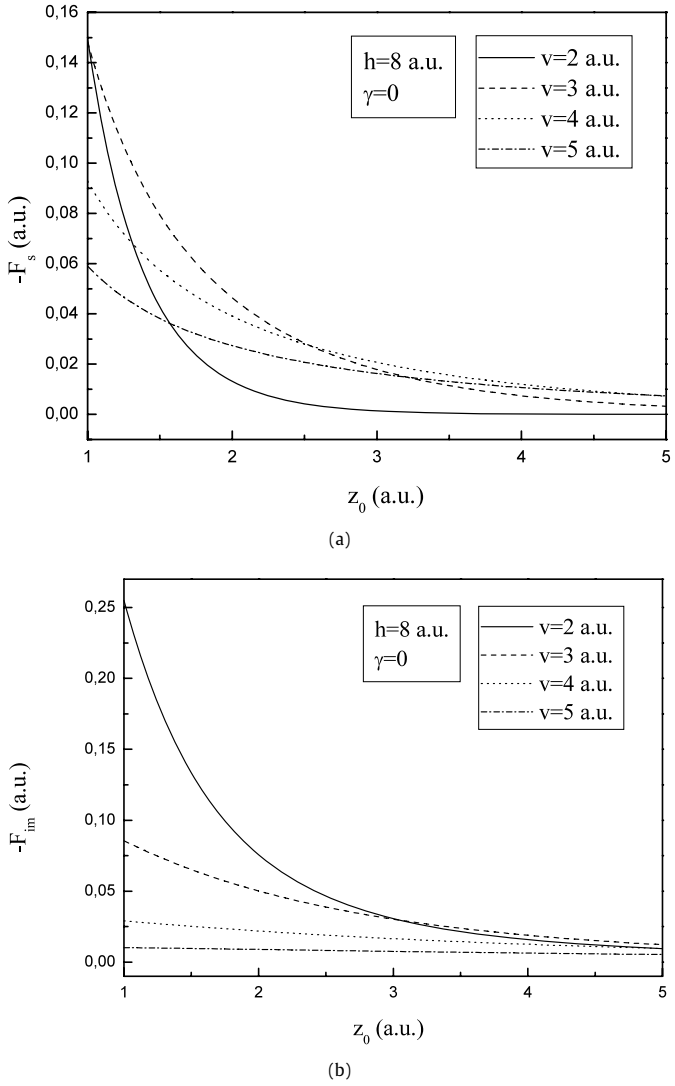

Fig. 2. The dependencies on distance z_0 (in a.u.) of (a) stopping and (b) image forces (in a.u.) on proton moving at speeds $v = 2$ a.u. (solid lines), 3 a.u. (dashed lines), 4 a.u. (dotted lines) and 5 a.u. (dash-dotted lines), above 2DEG with SiO_2 substrate (with $\varepsilon_s = 3.9$ and $h = 8$ a.u.), with zero damping $\gamma = 0$.

with the derivatives $\nabla_{\parallel}\Phi_{ind}(\vec{R}, z, t)$ and $\partial\Phi_{ind}(\vec{R}, z, t)/\partial z$ taken at the ion position ($\vec{R} = \vec{v}t, z = z_0$). Note that the stopping force is the negative of the usual stopping power S, $F_s = -S$, whereas the image force is related to the familiar image potential V_{im} of an ion by $F_{im} = -dV_{im}/dz_0$ [49].

For an ion of charge Q moving along the x axis with speed v at a fixed distance $z_0 > 0$ above a 2DEG, the stopping and the image forces are given by, respectively

$$F_s = \frac{2Q^2}{\pi}\int_0^{\infty}\int_0^{\infty}\frac{k_x e^{-2kz_0}}{k}\,\mathrm{Im}\left[\frac{1}{\varepsilon(k, k_x v)}\right]dk_x\,dk_y \tag{20}$$

$$F_{im} = -\frac{2Q^2}{\pi}\int_0^{\infty}\int_0^{\infty}e^{-2kz_0}\,\mathrm{Re}\left[1 - \frac{1}{\varepsilon(k, k_x v)}\right]dk_x\,dk_y \tag{21}$$

where we have used the symmetry properties of the real and imaginary parts of the dielectric function $\varepsilon(k, \omega)$ from Eq. (13).

In Fig. 1, we display the velocity dependencies of the (a) stopping and (b) image forces on proton ($Q = 1$) for several values of the gap h between 2DEG and a SiO_2 substrate (with $\varepsilon_s = 3.9$) at fixed distance $z_0 = 3$ a.u. with zero damping $\gamma = 0$. One notices that, when the velocity increases, both the stopping force and the image force increase in magnitude, pass through maxima after the speed $v = 2$ a.u. and monotonically decrease. Note that the velocity dependence of the stopping force exhibits a threshold at $v_{th} > \sqrt{\alpha} \approx 1.16$ a.u., characteristic of the plasmon excitation mechanism of energy loss, whereas the velocity dependence of the image force exhibits the significant tendency of saturation at the lowest and the highest speeds shown. However, the most remarkable features shown in Fig. 1 are the very strong dependencies of both forces on values of the 2DEG-substrate gap.

Fig. 2 shows the dependencies of the (a) stopping and (b) image forces on the proton-2DEG distance z_0 for several values of the speed v, and for the value of the gap $h = 8$ a.u., which is probably close to a typical experimental situation for 2DEG confined to a graphene sheet [33], with zero damping $\gamma = 0$. One notices a strong decrease in the magnitudes of both the stopping and image forces with increasing distances of proton from the 2DEG. The decay rates of both forces are strongly affected by the proton speed, in accordance with the results found for carbon nanotubes [11,12,50].

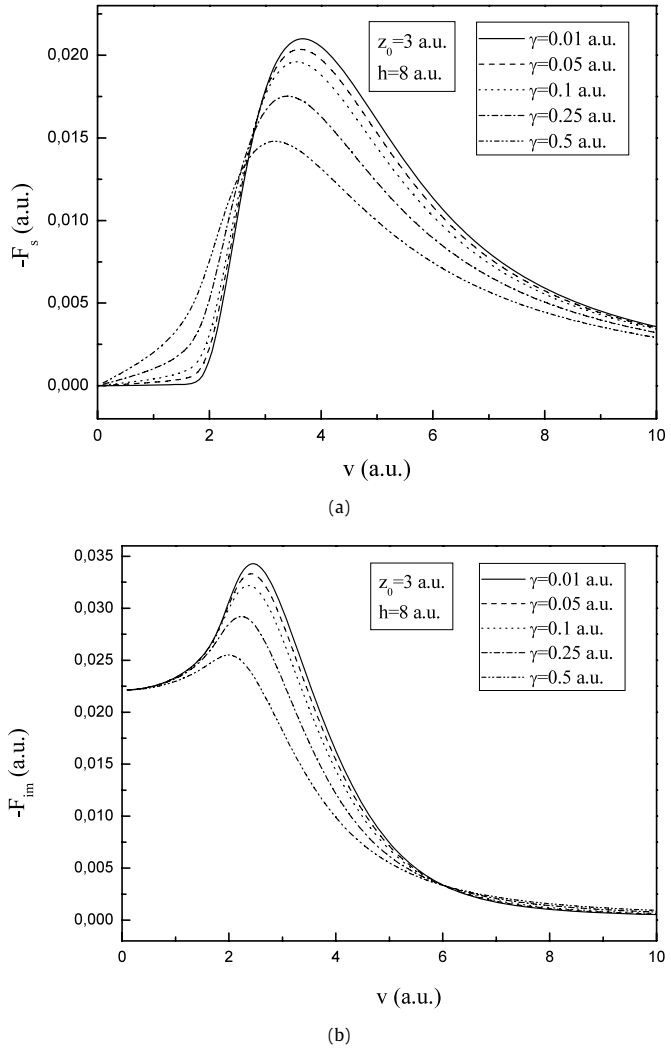

Fig. 3. The dependencies on speed v (in a.u.) of (a) stopping and (b) image forces (in a.u.) on proton moving at distance $z_0 = 3$ a.u. above 2DEG with SiO_2 substrate (with $\varepsilon_s = 3.9$ and $h = 8$ a.u.), for five values of damping, $\gamma = 0.01$ a.u. (solid lines), 0.05 a.u. (dashed lines), 0.1 a.u. (dotted lines), 0.25 a.u. (dash-dotted lines) and 0.5 a.u. (dash-dot-dotted lines).

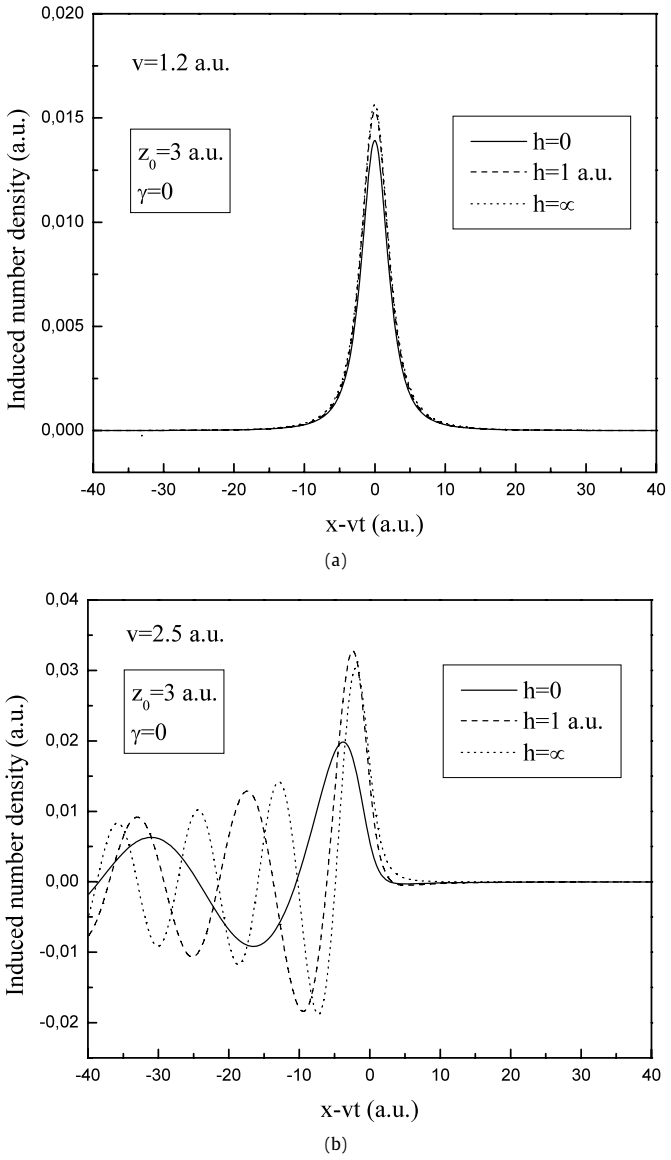

Fig. 4. The spatial distribution of the induced number density (in a.u.) along the projectile trail, for a proton moving along the x axis at distance $z_0 = 3$ a.u. above 2DEG for three values of the gap between 2DEG and a SiO_2 substrate (with $\varepsilon_s = 3.9$), $h = 0$ (solid lines), 1 a.u. (dashed lines) and ∞ (dotted lines), with zero damping $\gamma = 0$, at two speeds: (a) $v = 1.2$ a.u. and (b) $v = 2.5$ a.u.

In Fig. 3, we illustrate the effects of a finite frictional coefficient γ on the velocity dependencies of the (a) stopping and (b) image forces at fixed proton-2DEG distance $z_0 = 3$ a.u., and for the value of the gap $h = 8$ a.u. As expected, one notices the effect of smoothing out the resonant features in both forces around the speed $v = 2$ a.u., with little influences on their high-speed behaviours and on the low-speed behaviour of the image force. However, the low-speed values of the stopping force are noticeably dependent on γ, indicating that a threshold for energy loss to the plasmon excitations moves to lower speeds with increasing frictional coefficient.

Finally, Fig. 4 shows the spatial distribution of the induced number density for a proton moving along the x axis at distance $z_0 = 3$ a.u. above 2DEG, for several values of the gap h, with zero damping $\gamma = 0$, at two speeds: (a) $v = 1.2$ a.u. and (b) $v = 2.5$ a.u. In contrast to the wake effects for a charged particle moving above two-dimensional quantum electron gases [28], we study here the effects of variation in size of the 2DEG-substrate gap on the induced number density. Our calculations show that for all v values in the low-speed range, $0 < v \leqslant 1.2$, the induced number densities for different values of the gap h are practically on top of each other, as shown in Fig. 4(a) for the speed $v = 1.2$ a.u., describing a symmetrical, bell-shaped accumulation of the electrons in the 2DEG which screen the external charge. We found that the threshold for the wake effect depends on the values of the 2DEG-substrate gap and it moves to higher speeds with increasing gap h. In the range of speeds above the threshold for the collective excitations, our calculations show that the induced number density exhibits a development of the usual wake effect, which manifests in the oscillations trailing the proton ($x - vt < 0$), as shown in Fig. 4(b) for the speed $v = 2.5$ a.u. One can observe in Fig. 4(b) that the oscillation periods of the induced number density decrease when the values of the 2DEG-substrate gap increase.

In order to study the quantum diffraction (QD) effects coming from the quantum pressure, we have added the term $(1/4n_0)\nabla_\parallel \times [\nabla_\parallel^2 n(\vec{R}, t)]$, which describes the QD effects, in the right side of Eq. (8) and recalculated the stopping force, the image force and the induced number density.

In Fig. 5, we show the QD effects on the velocity dependencies of the (a) stopping and (b) image forces on proton moving at dis-

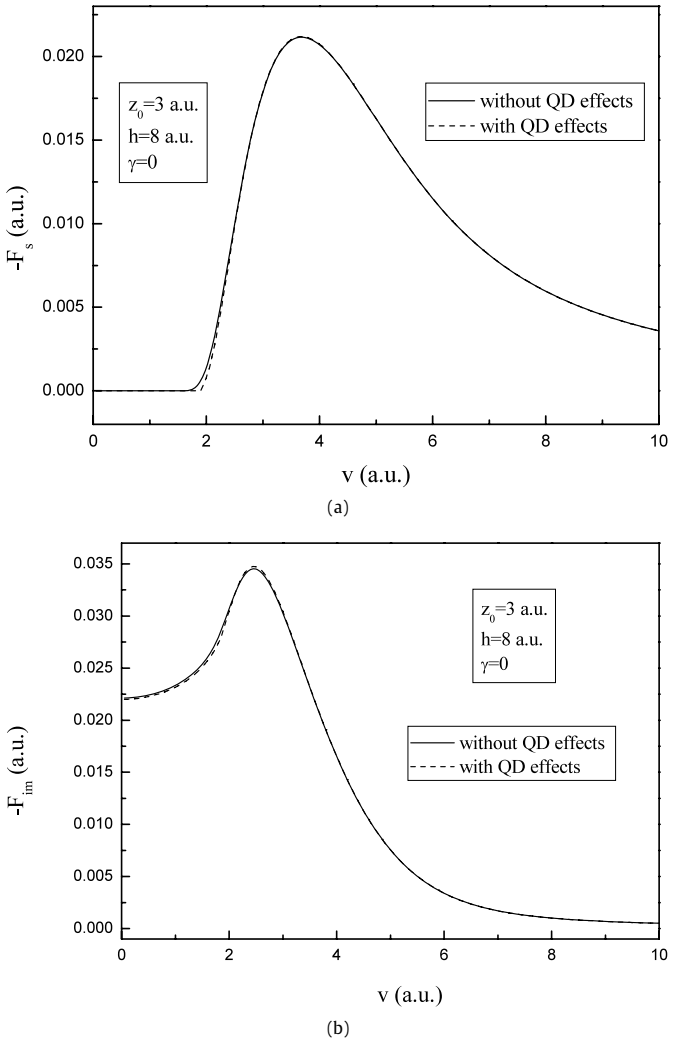

Fig. 5. The dependencies on speed v (in a.u.) of (a) stopping and (b) image forces (in a.u.) on proton moving at distance $z_0 = 3$ a.u. above 2DEG with SiO_2 substrate (with $\varepsilon_s = 3.9$ and $h = 8$ a.u.), with zero damping $\gamma = 0$, without QD effects (solid lines) and with QD effects (dashed lines).

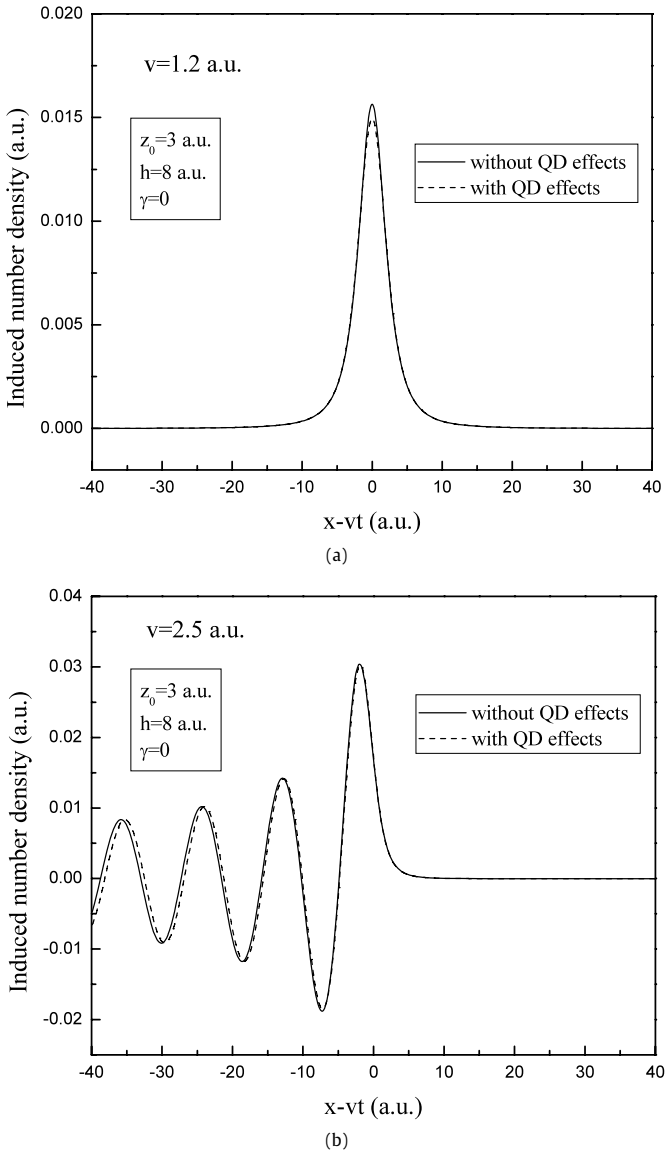

Fig. 6. The spatial distribution of the induced number density (in a.u.) along the projectile trail, for a proton moving along the x axis at distance $z_0 = 3$ a.u. above 2DEG with SiO_2 substrate (with $\varepsilon_s = 3.9$ and $h = 8$ a.u.), with zero damping $\gamma = 0$, without QD effects (solid lines) and with QD effects (dashed lines), at two speeds: (a) $v = 1.2$ a.u. and (b) $v = 2.5$ a.u.

tance $z_0 = 3$ a.u. above 2DEG with SiO_2 substrate (with $\varepsilon_s = 3.9$ and $h = 8$ a.u.), with zero damping $\gamma = 0$. Our calculations show that the QD effects have no influence on the image force, as shown in Fig. 5(b). We found only a very little influence around the threshold value for energy loss to the plasmon excitations on the velocity dependence of the stopping force, as shown in Fig. 5(a), but it can be neglected.

Fig. 6 shows the spatial distribution of the induced number density for a proton moving along the x axis at distance $z_0 = 3$ a.u. above 2DEG with SiO_2 substrate (with $\varepsilon_s = 3.9$ and $h = 8$ a.u.), with zero damping $\gamma = 0$, at two speeds: (a) $v = 1.2$ a.u. and (b) $v = 2.5$ a.u., with and without QD effects. One notices that QD effects have only a very little influence on the peak value, as shown in Fig. 6(a), which can be neglected and a negligible influence on the oscillation periods of the induced number density, as shown in Fig. 6(b).

4. Concluding remarks

We have used a 2D one-fluid hydrodynamic model to describe the high-frequency collective electron excitations in a 2DEG corresponding to the four valence electrons in graphene. Linearization of the hydrodynamic equations gives compact expressions for the induced potential, stopping force and the image force on charged particles moving parallel to the 2DEG supported by an insulating substrate, as well as for the induced number density per unit area of electrons in the 2DEG.

Numerical results show that the magnitudes of both the stopping and image forces exhibit typical resonance-shaped velocity dependencies, with the overall magnitudes decreasing sharply with increasing distances. When the velocity increases, both the stopping force and the image force increase in magnitude, pass through maxima and monotonically decrease. We have found sizeable effects of the decay rate, especially after the speed $v = 2$ a.u. The velocity dependence of the stopping force exhibits a threshold which moves to lower speeds with increasing frictional coefficient. The size of the 2DEG-substrate gap may exert quite large influence on the magnitudes of both the stopping and image forces on moving ions. When the particle speed exceeds a threshold value for the collective excitations, the induced number density shows usual wake oscillations. We have also found that the oscillation periods

of the induced number density decrease when the values of the 2DEG-substrate gap increase. Finally, we have found that the QD effects in the case of a 2DEG with the parameters characteristic of graphene have a very little influence on the interaction process, which can be neglected.

Acknowledgements

This work has been supported by the Ministry of Science and Technological Development of the Republic of Serbia (Project No. 141013). The authors are most grateful to Professor Zoran L. Mišković, Dr. Ljupčo Hadžievski and Dr. Nataša Bibić for many useful comments and continuing support.

References

[1] K.S. Novoselov, A.K. Geim, S.V. Morozov, D. Jiang, Y. Zhang, S.V. Dubonos, I.V. Grigorieva, A.A. Firsov, Science 306 (2004) 666.
[2] A.H. Castro Neto, F. Guinea, N.M.R. Peres, K.S. Novoselov, A.K. Geim, Rev. Mod. Phys. 81 (2009) 109.
[3] A.K. Geim, P. Kim, Sci. Am. 298 (2008) 90.
[4] C. Kramberger, R. Hambach, C. Giorgetti, M.H. Rümmeli, M. Knupfer, J. Fink, B. Büchner, L. Reining, E. Einarsson, S. Maruyama, F. Sottile, K. Hannewald, V. Olevano, A.G. Marinopoulos, T. Pichler, Phys. Rev. Lett. 100 (2008) 196803.
[5] T. Eberlein, U. Bangert, R.R. Nair, R. Jones, M. Gass, A.L. Bleloch, K.S. Novoselov, A.K. Geim, P.R. Briddon, Phys. Rev. B 77 (2008) 233406.
[6] G. Ramos, B.M.U. Scherzer, Nucl. Instrum. Methods B 85 (1994) 479.
[7] G. Ramos, B.M.U. Scherzer, Nucl. Instrum. Methods B 174 (2001) 329.
[8] E. Yagi, T. Iwata, T. Urai, K. Ogiwara, J. Nucl. Mater. 334 (2004) 9.
[9] S. Cernusca, M. Fürsatz, H.P. Winter, F. Aumayr, Europhys. Lett. 70 (2005) 768.
[10] T. Kaneko, H. Kudo, S. Tomita, R. Uchiyama, J. Phys. Soc. Jpn. 75 (2006) 034717.
[11] D.J. Mowbray, Z.L. Mišković, F.O. Goodman, Y.-N. Wang, Phys. Rev. B 70 (2004) 195418.
[12] D.J. Mowbray, Z.L. Mišković, F.O. Goodman, Phys. Rev. B 74 (2006) 195435.
[13] D. Borka, S. Petrović, N. Nešković, D.J. Mowbray, Z.L. Mišković, Phys. Rev. A 73 (2006) 062902.
[14] T. Fauster, M. Weinelt, V. Hofer, Prog. Surf. Sci. 82 (2007) 224.
[15] M. Zamkov, N. Woody, S. Bing, H.S. Chakraborty, Z. Chang, U. Thumm, P. Richard, Phys. Rev. Lett. 93 (2004) 156803.
[16] A.L. Fetter, Ann. Phys. 81 (1973) 367.
[17] T. Stockli, J.M. Bonard, A. Chatelain, Z.L. Wang, P.A. Stadelmann, Phys. Rev. B 64 (2001) 115424.
[18] J. Zuloaga, Z.L. Mišković, F.O. Goodman, Nucl. Instrum. Methods B 256 (2007) 162.
[19] I. Radović, Lj. Hadžievski, N. Bibić, Z.L. Mišković, Phys. Rev. A 76 (2007) 042901.
[20] I. Radović, Lj. Hadžievski, N. Bibić, Z.L. Mišković, Mater. Chem. Phys. 118 (2009) 293.
[21] D. Borka, D.J. Mowbray, Z.L. Mišković, S. Petrović, N. Nešković, Phys. Rev. A 77 (2008) 032903.
[22] D. Borka, D.J. Mowbray, Z.L. Mišković, S. Petrović, N. Nešković, J. Phys.: Condens. Matter 20 (2008) 474212.
[23] J. Neufeld, R.H. Ritchie, Phys. Rev. 98 (1955) 1632.
[24] L.-J. Hou, Y.-N. Wang, Z.L. Mišković, Phys. Rev. E 68 (2003) 016410.
[25] Y.-N. Wang, H.-T. Qiu, Z.L. Mišković, Phys. Rev. Lett. 85 (2000) 1448.
[26] N.R. Arista, Phys. Rev. A 64 (2001) 032901.
[27] D.J. Mowbray, Z.L. Mišković, F.O. Goodman, Y.-N. Wang, Phys. Lett. A 329 (2004) 94.
[28] C.-Z. Li, Y.-H. Song, Y.-N. Wang, Phys. Lett. A 372 (2008) 4500.
[29] C.-Z. Li, Y.-H. Song, Y.-N. Wang, Chin. Phys. Lett. 25 (2008) 2981.
[30] C.-Z. Li, Y.-H. Song, Y.-N. Wang, Phys. Rev. A 79 (2009) 062903.
[31] J. Burgdörfer, Nucl. Instrum. Methods B 67 (1992) 1.
[32] G. Bertoni, L. Calmels, A. Altibelli, V. Serin, Phys. Rev. B 71 (2005) 075402.
[33] M. Ishigami, J.H. Chen, W.G. Cullen, M.S. Fuhrer, E.D. Williams, Nano Lett. 7 (2007) 1643.
[34] E.H. Hwang, S. Das Sarma, Phys. Rev. B 75 (2007) 205418.
[35] B. Wunsch, T. Stauber, F. Sols, F. Guinea, New J. Phys. 8 (2006) 318.
[36] I. Radović, Lj. Hadžievski, Z.L. Mišković, Phys. Rev. B 77 (2008) 075428.
[37] K.F. Allison, D. Borka, I. Radović, Lj. Hadžievski, Z.L. Mišković, Phys. Rev. B 80 (2009) 195405.
[38] A.K. Geim, A.H. MacDonald, Phys. Today (August 2007) 35.
[39] A. Moradi, Phys. Lett. A 372 (2008) 5614.
[40] A. Moradi, Physica E 41 (2009) 1338.
[41] C.-Z. Li, Y.-H. Song, Y.-N. Wang, Nucl. Instrum. Methods B 267 (2009) 3129.
[42] D.J. Mowbray, Ph.D. Thesis, University of Waterloo, Ontario, Canada, 2007.
[43] E. Prodan, C. Radloff, N.J. Halas, P. Nordlander, Science 302 (2003) 419.
[44] T.P. Doerr, Y.K. Yu, Am. J. Phys. 72 (2004) 190.
[45] B.P. van Zyl, E. Zaremba, Phys. Rev. B 59 (1999) 2079.
[46] R.G. Parr, W. Yang, Density-Functional Theory of Atoms and Molecules, Oxford University Press, New York, 1989.
[47] M. Nakayama, J. Phys. Soc. Jpn. 36 (1974) 393.
[48] A.L. Fetter, Ann. Phys. 88 (1974) 1.
[49] J.M. Pitarke, V.M. Silkin, E.V. Chulkov, P.M. Echenique, Rep. Prog. Phys. 70 (2007) 1.
[50] Y.-N. Wang, Z.L. Mišković, Phys. Rev. A 69 (2004) 022901.